

Fig. 4. Inactivation of an MCM protein after the activation of early origins of DNA replication blocks S-phase progression irreversibly. Cells were grown in the medium YP+Galactose. (A) Samples were taken throughout the experiment to make protein extracts, and the levels of Mcm4-td and Ubr1 were determined by immunoblot analysis [for details of antibodies, see (11)]. The loading control shows Ponceau S staining of a portion of the membrane used to detect Mcm4-td, between the 200 and 97 kD

markers. (B) Cell viability was determined during the experiment described in (A) by plating cells on YPD (YP+dextrose) plates and counting the number of colonies after 2 days of incubation at 24°C. (C) At the end of the experiment described in (A), cells were released from α factor arrest [(i) and (ii)] and hydroxyurea arrest [(iii) and (iv)], and incubation was continued in fresh medium at 24°C for the indicated times. DNA content was monitored by flow cytometry.

Essential Role for Cholesterol in Entry of Mycobacteria into Macrophages

John Gatfield and Jean Pieters*

Mycobacteria are intracellular pathogens that can invade and survive within host macrophages, thereby creating a major health problem worldwide. The molecular mechanisms involved in mycobacterial entry are still poorly characterized. Here we report that cholesterol is essential for uptake of mycobacteria by macrophages. Cholesterol accumulated at the site of mycobacterial entry, and depleting plasma membrane cholesterol specifically inhibited mycobacterial uptake. Cholesterol also mediated the phagosomal association of TACO, a coat protein that prevents degradation of mycobacteria in lysosomes. Thus, by entering host cells at cholesterol-rich domains of the plasma membrane, mycobacteria may ensure their subsequent intracellular survival in TACO-coated phagosomes.

Macrophages play an important role in the host defense against bacteria because of their capacity to phagocytose and to degrade microbes in lysosomes. Mycobacteria, which are highly successful pathogens, resist delivery to lysosomes and instead survive within a

specialized vacuole, the mycobacterial phagosome (1–3). The bacteria survive intracellularly because they are able to actively recruit and retain TACO (for tryptophane aspartate-containing coat protein) at the mycobacterial phagosome, where it prevents fu-

sion of phagosomes with lysosomes (4). TACO lacks a putative transmembrane domain, which suggests that it is a peripherally associated protein. To analyze the association of TACO with the phagosomal membrane, murine macrophages were infected with *Mycobacteria bovis* Bacille Calmette-Guérin (BCG). Subjection of isolated phagosomes to conditions known to release membrane-associated proteins, such as high salt (1 M NaCl), sodium carbonate (pH 11), and Triton X-100 (1%), did not solubilize TACO (Fig. 1A), although some background release was apparent because of the fragility of isolated phagosomes. However, extraction of the phagosomes in 0.02% digitonin, a cholesterol-sequestering reagent (5), resulted in complete solubilization of TACO, to the same degree as disruption of the phagosomes in SDS or urea (Fig. 1A). Similarly, digitonin, but not Triton X-100, disrupted TACO association with membranes from uninfected cells

Basel Institute for Immunology, Grenzacherstrasse 487, CH-4005 Basel, Switzerland.

*To whom correspondence should be addressed. E-mail: pieters@bii.ch

REPORTS

(Fig. 1C). Furthermore, in cells depleted of cholesterol (6), TACO was not associated with the membrane fraction (Fig. 1D). TACO was completely solubilized after Triton X-100 treatment at 25°C (Fig. 1E), which suggests that incomplete extraction was not because of cytoskeletal association (7). Thus, TACO is associated with membranes in a cholesterol-dependent manner.

To analyze the distribution of cholesterol during phagocytosis, macrophages that had taken up *M. bovis* BCG expressing the green fluorescent protein (GFP) (8) for 1 hour, followed by a 2.5-hour chase, were fixed and analyzed by fluorescence microscopy. Cholesterol was visualized by using the cholesterol-binding compound filipin (9, 10). Whereas in uninfected macrophages cholesterol was distributed at the plasma membrane, as well as in intracellular stores (Fig. 1B), infection of macrophages with mycobacteria resulted in relocation and accumulation of cholesterol at the site of bacterial entry in all phagocytosing cells examined (Fig. 1B).

To further analyze the role of cholesterol in mycobacterial uptake, cellular cholesterol levels were reduced by pharmacological inhibition of cholesterol synthesis followed by

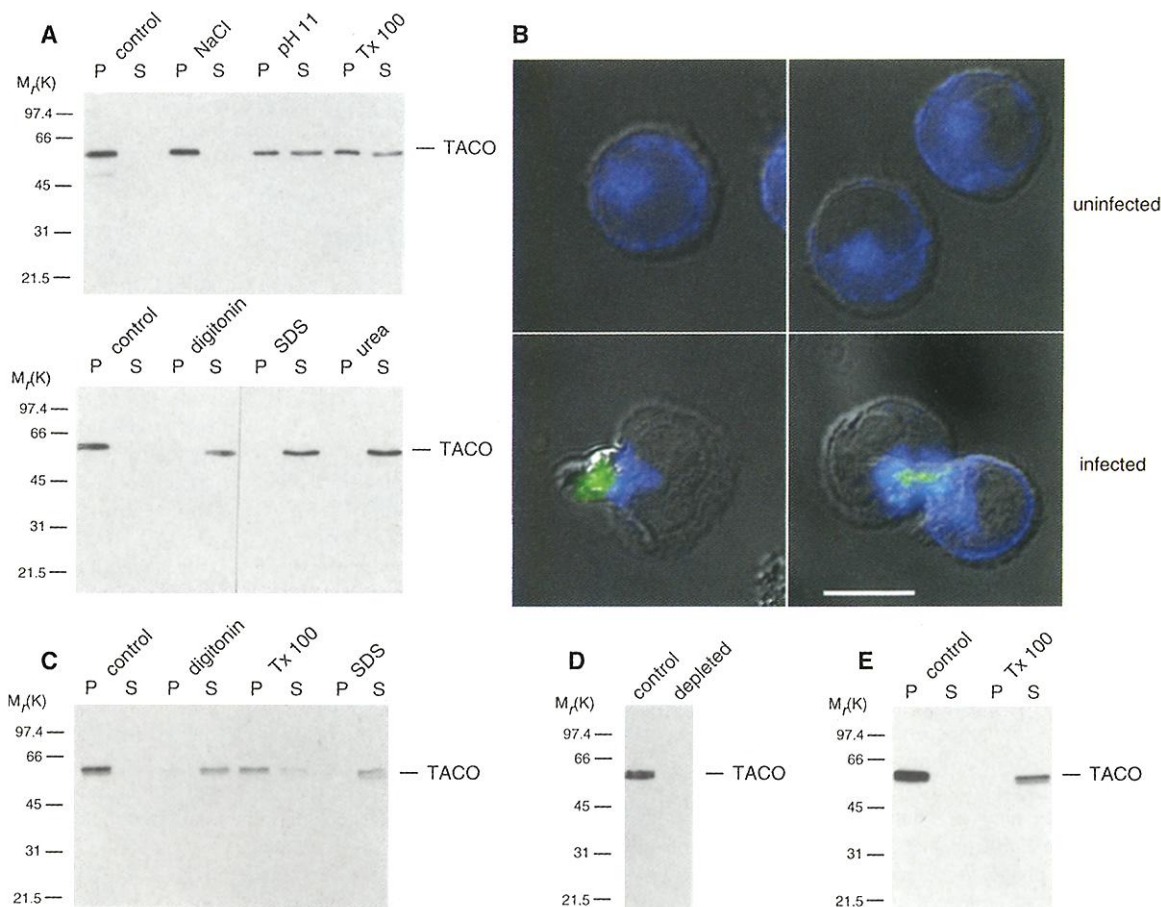
extraction of residual cholesterol from the plasma membrane (6). Cholesterol depletion led to a specific decrease in total cellular cholesterol levels (~60 to 70%) as determined by thin-layer chromatography (TLC) and densitometry (Fig. 2, C and D). Cholesterol-depleted macrophages were infected with metabolically labeled *M. bovis* BCG, and the degree of uptake was analyzed. Depletion of plasma membrane cholesterol resulted in a reduction of mycobacterial uptake of ~85 to 90% by both the macrophage cell line J774A.1 and bone marrow-derived macrophages (Fig. 2A). In addition, cholesterol depletion caused a similar reduction of *M. tuberculosis* uptake of ~85% (Fig. 2B). To test whether inhibition of uptake was specific for mycobacteria or occurred as a result of a general inhibition of all phagocytic events, the ability of depleted macrophages to phagocytose various other microorganisms was analyzed. Depleted macrophages were still capable of internalizing *Escherichia coli*, *Yersinia pseudotuberculosis*, *Salmonella typhimurium*, and *Lactobacillus casei* (Fig. 2B).

To visualize phagocytosis events in normal and cholesterol-depleted macrophages, cells were followed by time-lapse video microscopy after the addition of bacteria.

Mycobacteria were readily phagocytosed by control macrophages (Fig. 3A and see video at www.bii.ch/pieters/movies.html), whereas depletion of cellular cholesterol resulted in an abrogation of mycobacterial uptake (Fig. 3A and see video). Instead of being internalized, the bacilli became loosely associated with macrophage membranes (Fig. 3A). Quantification of phagocytic events observed after video microscopy revealed that the percentage of phagocytosing cells was reduced to ~15% after cholesterol depletion (Fig. 3B).

As cholesterol is involved in the regulation of membrane fluidity (11, 12), depletion may affect other cellular functions besides mycobacterial uptake. To analyze whether depletion of surface cholesterol caused a general malfunctioning of the plasma membrane, the overall motility, as well as the membrane ruffling, of control and depleted cells was analyzed. All cells under control and cholesterol-depleted conditions showed membrane ruffling (Fig. 3C), although qualitative differences were apparent, most likely because of altered membrane fluidity (see video). Consistent with a role for cholesterol in providing rigidity to the cell surface (12), cellular

Fig. 1. Association of TACO with the (A) phagosomal and (C through E) plasma membrane. Phagosomes (A) or membranes (C through E) were isolated from J774A.1 macrophages as described (4, 24, 25) and incubated in extraction buffer (20 mM HEPES, pH 7, 5 mM MgCl₂, and 100 mM NaCl) supplemented as indicated for 30 min at 4°C (A, C, and D) or 25°C (E). After sedimentation at 20,000g for 15 min, pellets (P) and supernatants (S) were analyzed for the presence of TACO by SDS-polyacrylamide gel electrophoresis (10%) and immunoblotting. (B) Distribution of cholesterol during mycobacterial uptake. J774A.1 macrophages were incubated with *M. bovis* BCG expressing GFP (26) for 1 hour, washed, and chased for an additional 2 hours. Cholesterol was localized after fixation of the cells in 3% paraformaldehyde at 37°C for 10 min followed by incubation in 0.05% (w/v) filipin (blue) (Sigma) (10) in PBS for 4 hours at room temperature. Scale bar, 10 μm.



REPORTS

motility was moderately enhanced after cholesterol depletion (Fig. 3D). In addition, the effect of cholesterol depletion on protein biosynthesis was analyzed and found to be equal in control and depleted cells (Fig. 3E).

To better understand the role of cholesterol in mycobacterial entry, the receptor molecules involved were analyzed. Whereas mannan did not block mycobacterial uptake (13),

antibodies against complement receptor type 3 (anti-CR3) (14–17) blocked the entry of mycobacteria into J774A.1 cells, as well as into bone marrow–derived macrophages (Fig. 4A). To define the role of cholesterol in CR3-mediated uptake per se, macrophages were depleted of cholesterol and the capacity of control and depleted macrophages to phagocytose *L. casei* in a CR3-dependent manner was analyzed. Cholesterol-depleted

and control cells showed an equal capacity to internalize *L. casei*, and the uptake of *L. casei* in both depleted and control macrophages was inhibited by anti-CR3 antibodies (Fig. 4B). Thus, cholesterol is not required for complement receptor function in general but specifically for mycobacterial entry.

Because cholesterol is not required for complement receptor function, but is nevertheless crucial for mycobacterial entry

Fig. 2. Effect of cholesterol depletion on mycobacterial entry. (A) Control (black bars) and cholesterol-depleted (6) (gray bars) subconfluent monolayers of J774 cells or bone marrow–derived macrophages (BMM) (27) were infected with metabolically labeled *M. bovis* BCG ($OD_{600} = 3$ in DMEM) for 1 hour, followed by a 2.5-hour chase, after which the cell-associated radioactivity was determined. The relative amount of uptake was determined by dividing counts per minute by the cell number in every sample. Results shown represent mean values (\pm SD) from three experiments and are corrected for background adherence occurring at 4°C. Au, arbitrary units. (B) Control and cholesterol-depleted J774 cells were allowed to internalize the different GFP-expressing ($OD_{600} = 2$) or metabolically labeled ($OD_{600} = 3$) microorganisms (28). Phagocytosis was corrected for background adherence in the cold and is expressed as percent phagocytosed bacilli compared with macrophages that were not depleted. (C and D) Analysis of cholesterol content in control and depleted J774 macrophages by TLC (C) and fluorescence microscopy (D). TLC analysis was performed as described (29), and visualized using 3% cupric acetate in 15% aqueous phosphoric acid and exposure of the TLC plate at 120°C for 1 hour.

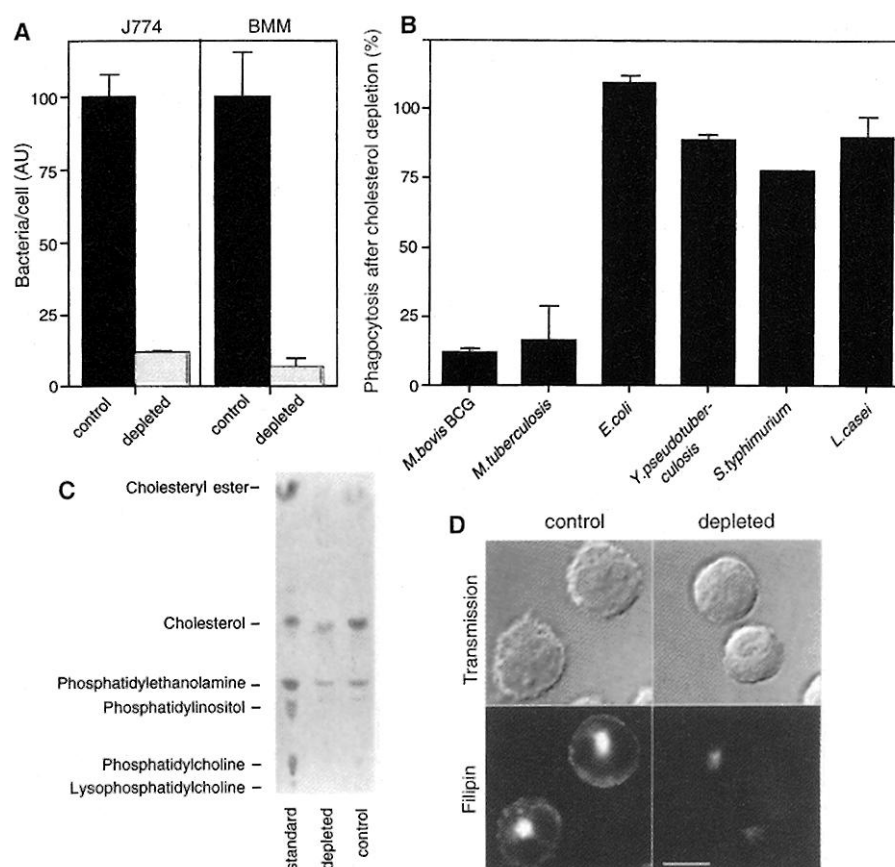
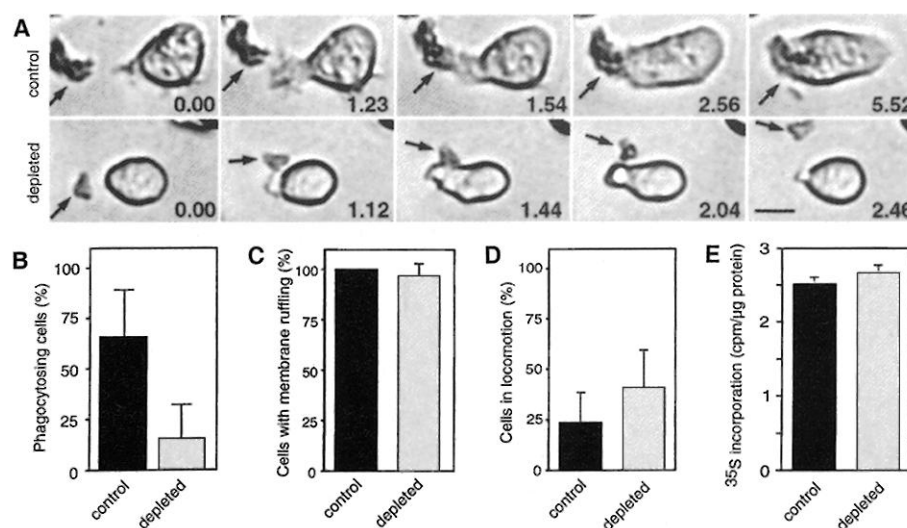


Fig. 3. Time-lapse video microscopy. Control and cholesterol-depleted J774 macrophages grown to 20% confluency were incubated with mycobacteria ($OD_{600} = 0.1$), and 1-hour sequences were recorded by video microscopy using a digital camera (Hamamatsu Photonics, Japan) connected to a Zeiss Axiophot equipped with a thermostated (37°C) and CO₂ (5%) equilibrated chamber and OpenLab software (version 2.0). (A) Example of a phagocytic event from control (upper panels) and cholesterol-depleted (lower panels) macrophages. Bacteria are indicated by arrows. Time points are indicated in minutes, seconds. Scale bar, 10 μ m. Full video sequences can be accessed at www.bii.ch/pieters/movies.html. (B) Quantification of phagocytic events (control, 95 cells recorded from seven sequences; depleted, 89 cells recorded from eight sequences). Shown are mean values (\pm SD). (C and D) Effect of cholesterol depletion on membrane ruffling (C) and cell locomotion (D) determined from the sequences used in (B). Active movement of cells over a distance of 50 μ m within 1 hour was considered locomotion. (E) Protein biosynthesis in control and cholesterol-depleted J774 cells. Cells were metabolically labeled for 1 hour with [³⁵S]methionine and cysteine, washed, and lysed as described (30). Shown are mean values (\pm SD) from three experiments.



REPORTS

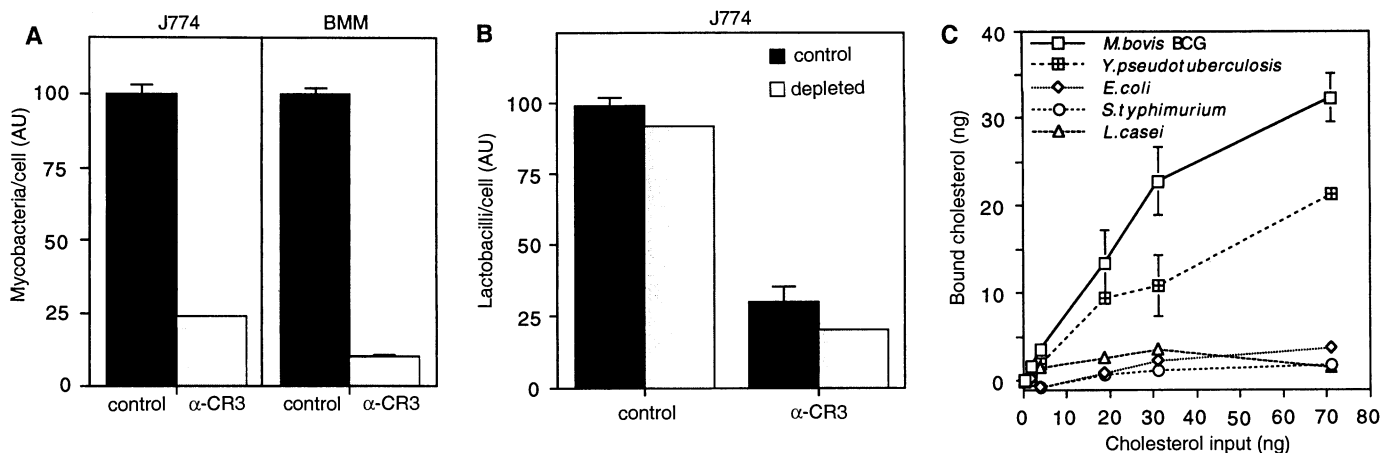


Fig. 4. (A) Effect of anti-CR3 antibodies (Serotec) on uptake of metabolically labeled mycobacteria by J774 and bone marrow–derived macrophages (BMM). (B) Effect of cholesterol depletion on CR3-mediated uptake of serum opsonized GFP-expressing lactobacilli by J774 macrophages. Cells were preincubated with the anti-CR3 antibodies for 10 min followed by the addition of bacteria for a period of 40 min. AU, arbitrary units. In (A) monoclonal antibodies M1/70 and 5C6 (80 μg/ml each) were used as a mixture; in (B) only 5C6 (20 μg/ml) was tested. (C) Cholesterol

binding capacity of various bacteria. Bacteria (6×10^6) were incubated with the indicated amounts of [4 - 14 C]cholesterol (NEN Life Sciences) for 1 hour at room temperature in 400 μl of DMEM. Bound and free cholesterol were separated by centrifugation of the bacterial suspensions through 0.5 M sucrose cushions, and the amount of cholesterol associated with the bacterial pellets was determined by liquid scintillation counting. Shown are mean values (\pm SD) from two experiments corrected for background values from samples without bacteria.

into macrophages, we next explored the possibility that mycobacteria could directly bind to cholesterol. Mycobacteria displayed a high binding capacity for cholesterol (Fig. 4C), whereas none of the other microorganisms analyzed displayed a similar binding of cholesterol, with the exception of *Yersinia*; the significance of this affinity is presently unclear, as cholesterol does not play a role in *Yersinia* uptake (Fig. 2B).

Together, our results indicate that plasma membrane cholesterol is required for a stable physical interaction of the mycobacteria with the plasma membrane, as a result of which the mycobacteria can be efficiently internalized. What may be the benefit of cholesterol-mediated entry for mycobacteria? Because TACO associates with the phagosomal membrane in a cholesterol-dependent manner, mycobacteria that enter macrophages at cholesterol-containing plasma membrane domains are subsequently sequestered in TACO-coated phagosomes, preventing lysosomal delivery and ensuring intracellular survival.

One of the hallmarks of mycobacteria is the extremely glycolipid-rich cell wall (18), which may contain compounds involved in cholesterol-mediated entry into macrophages. The availability of a blueprint for the biochemical pathways operating in *M. tuberculosis* through the elucidation of its complete genome sequence (19, 20) might allow the identification of components that may prove to be targets for anti-mycobacterial reagents.

References and Notes

1. C. J. Murray and J. A. Salomon, *Proc. Natl. Acad. Sci. U.S.A.* **95**, 13881 (1998).
 2. D. G. Russell, S. Sturgill-Koszycki, T. Vanheyningen, H.

Collins, U. E. Schaible, *Philos. Trans. R. Soc. London B. Biol. Sci.* **352**, 1303 (1997).
 3. B. R. Bloom, *Nature* **358**, 538 (1992).
 4. G. Ferrari, M. Naito, H. Langen, J. Pieters, *Cell* **97**, 435 (1999).
 5. T. K. Ray, J. Nandi, A. Dannemann, G. B. Gordon, *J. Cell Biochem.* **21**, 141 (1983).
 6. J774 and bone marrow–derived macrophages were depleted of cholesterol as described [M. Simons *et al.*, *Proc. Natl. Acad. Sci. U.S.A.* **95**, 6460 (1998)], with the following modifications: J774 cells were first cultured (at 37°C) for 60 hours in lovastatin (4 μM, Calbiochem) and mevalonate (250 μM, Sigma), followed by a 45-min treatment at 37°C by methyl-β-cyclodextrin (10 mM, Sigma) in serum-free Dulbecco's modified essential medium (DMEM) in the continuous presence of lovastatin and mevalonate. Bone marrow–derived macrophages were depleted for 180 hours in lovastatin and mevalonate, and residual cholesterol was extracted for 75 min with 20 mM methyl-β-cyclodextrin.
 7. K. Simons and E. Ikonen, *Nature* **387**, 569 (1997).
 8. S. Dhandayuthapani *et al.*, *Mol. Microbiol.* **17**, 901 (1995).
 9. H. Bornig and G. Geyer, *Acta Histochem.* **50**, 110 (1974).
 10. W. Drabikowski, E. Lagwinska, M. G. Sarzala, *Biochim. Biophys. Acta* **291**, 61 (1973).
 11. A. A. Spector and M. A. Yorek, *J. Lipid Res.* **26**, 1015 (1985).
 12. P. L. Yeagle, *Biochim. Biophys. Acta* **822**, 267 (1985).
 13. J. Gatfield and J. Pieters, unpublished results.
 14. E. J. Brown, *Curr. Opin. Immunol.* **3**, 76 (1991).
 15. C. Cywes, H. C. Hoppe, M. Daffe, M. R. Ehlers, *Infect. Immun.* **65**, 4258 (1997).
 16. R. W. Stokes, I. D. Haidl, W. A. Jefferies, D. P. Speert, *J. Immunol.* **151**, 7067 (1993).
 17. L. S. Schlesinger, *Curr. Top. Microbiol. Immunol.* **215**, 71 (1996).
 18. P. J. Brennan and H. Nikaido, *Annu. Rev. Biochem.* **64**, 29 (1995).
 19. S. T. Cole *et al.*, *Nature* **393**, 537 (1998).
 20. D. B. Young, *Nature* **393**, 515 (1998).
 21. R. H. Valdivia, A. E. Hromockyj, D. Monack, L. Ramakrishnan, S. Falkow, *Gene* **173**, 47 (1996).
 22. R. H. Valdivia and S. Falkow, *Science* **277**, 2007 (1997).
 23. C. Efthymiou and P.A. Hansen, *J. Infect. Dis.* **110**, 258 (1962).
 24. A. Tulp, D. Verwoerd, B. Dobberstein, H. L. Ploegh, J. Pieters, *Nature* **369**, 120 (1994).

25. Z. Hasan *et al.*, *Mol. Microbiol.* **24**, 545 (1997).
 26. *Mycobacterium bovis* BCG, strain Montreal, was kindly provided by J. Thole. *M. bovis* BCG was metabolically labeled by incubation in 1.5 μCi/ml [35 S]methionine/cysteine (Promix, Amersham) for 12 hours at 37°C. *M. bovis* BCG harboring *phsp60-gfp* (8) was kindly provided by V. Deretic. *M. tuberculosis* strain H37Rv was kindly donated by B. Heym. Mycobacteria were propagated in 7H9 mycobacterial medium (Difco) supplemented with 10% OADC Middlebrook supplement (Difco).
 27. Bone marrow–derived macrophages were generated by incubating bone marrow cells from C57BL/6 mice for 7 days in DMEM containing 10% heat-inactivated fetal calf serum, 5% inactivated horse serum, penicillin and streptomycin, 2 mM L-glutamine, 1 mM sodium pyruvate, 0.1 mM 2-mercaptoethanol, and 30% L-929-conditioned medium.
 28. *Salmonella typhimurium* expressing GFPmut3 (21, 22) (kind gift from S. Falkow and R. Valdivia) and *E. coli* strain BL21 expressing GFP (gift from A. Dijkstra) were cultured in Luria Bertani (LB) medium at 37°C. *Y. pseudotuberculosis* expressing GFPmut3 (gift from S. Falkow and R. Valdivia) was grown in 2× YT medium at 37°C. GFP-expressing *L. casei* (kind gift from M. Shaw) was cultured as described (23). Control or cholesterol-depleted cells were incubated at 37°C or left on ice with the indicated GFP-expressing microorganisms ($OD_{600} = 2$) for 40 min, washed and fixed in 1% paraformaldehyde followed by analysis by flow cytometry. The degree of phagocytosis was calculated from the percentage of phagocytosing cells under control and depleted conditions. For opsonized *L. casei*, washed bacteria were incubated in 10% fresh human serum in DMEM (at $OD_{600} = 2$) for 1 hour at 37°C and washed twice before use.
 29. J. Bramham and F. G. Riddell, *J. Inorg. Biochem.* **57**, 23 (1995).
 30. J. Pieters, H. Horstmann, O. Bakke, G. Griffiths, J. Lipp, *J. Cell Biol.* **115**, 1213 (1991).
 31. We thank V. Deretic, A. Dijkstra, S. Falkow, R. Valdivia, M. Shaw, and J. Thole for strains and reagents; M. Dessing, S. Meyer, and A. Traunecker for assistance with (video) microscopy; M. Adler for allowing access to P3 facilities; and T. Harder, M. Kopf, and W. Philipp for comments on the manuscript. The Basel Institute for Immunology was founded and is supported by Hoffmann–La Roche Ltd., Basel, Switzerland.

23 December 1999; accepted 7 April 2000